J. Synchrotron Rad. (1998). **5**, 1114–1116

X-ray microprobe system for XRF analysis and spectroscopy at SPring-8 BL39XU

Shinjiro Hayakawa,[a]* Shunji Goto,[b] Takashi Shoji,[c] Eiji Yamada[c] and Yohichi Gohshi[a]

[a]*Department of Applied Chemistry, School of Engineering, The University of Tokyo, Hongo, Bunkyo, Tokyo 113, Japan,* [b]*JASRI, SPring-8, Kamigori, Hyogo 678-12, Japan, and* [c]*RIGAKU Industrial Corporation, Takatsuki, Osaka 569, Japan. E-mail: thaya@hongo.ecc.u-tokyo.ac.jp*

(*Received 4 August 1997; accepted 8 December 1997*)

An X-ray microprobe system for X-ray fluorescence (XRF) analysis and spectroscopy has been developed at SPring-8 BL39XU; it comprises an X-ray focusing or collimation system, energy-dispersive (ED) and wavelength-dispersive (WD) XRF spectrometers, and a sample-scanning system. The conventional ED spectrometer will be utilized for qualitative and quantitative trace-element analysis, and the WD spectrometer will be used both for trace-element analysis and XRF spectroscopy. A combination of monochromated undulator radiation and the WD spectrometer will enable resonant XRF spectroscopy using brilliant hard X-ray undulator radiation.

Keywords: X-ray fluorescence; SPring-8; wavelength-dispersive spectrometers; trace-element analysis.

1. Introduction

X-ray analyses have made great progress utilizing synchrotron radiation owing to its unique characteristics, such as high brilliance, small divergence and energy tunability. In the field of X-ray fluorescence (XRF) analysis the detection limit using an energy-dispersive (ED) spectrometer has reached less than 1 p.p.m. for most of the transition elements, and X-ray absorption fine structure (XAFS) measurements using the XRF method provide chemical state or local structural information on trace elements. Innovations in X-ray focusing optics have made it possible to construct a hard X-ray microprobe with a spatial resolution of around 1 µm (Hayakawa *et al.*, 1989) and the characterization of trace elements has been realized using an energy-tunable X-ray microprobe (Hayakawa & Gohshi, 1996). In addition to trace-element analysis, high-resolution XRF spectroscopy has received great attention. In the soft X-ray region profile changes or resonant effects of XRF spectra have been investigated intensively by changing the incident beam energy around the absorption edge of the element of interest. However, very few experimental results (Ohashi *et al.*, 1992; Hamalainen *et al.*, 1992) have been reported in the hard X-ray region because the production of undulator radiation was difficult with second-generation synchrotron radiation sources.

Utilizing the hard X-ray undulator at SPring-8 an extremely high photon-flux density can be expected on samples, and good counting statistics can be expected even with a high-resolution XRF spectrometer. Moreover, owing to the extremely small divergence of the undulator radiation, a perfect-crystal phase retarder (Hirano *et al.*, 1993) can be effectively used to control the polarization of the incident X-ray beam. This paper describes the energy-tunable X-ray microprobe system for XRF analysis and spectroscopy at SPring-8 on the BL39XU beamline.

2. Outline of BL39XU

BL39XU is equipped with an in-vacuum-type linear undulator which comprises 140 sets of permanent magnets whose period (λ_u) is 32 mm (Kitamura, 1994). The tunable range of the undulator gap is from 8 to 50 mm, and covers undulator radiation from 5 to 25 keV by utilizing the first and third harmonics. A brilliance of more than 1×10^{19} photons s^{-1} $mrad^{-2}$ mm^{-1} (0.1% bandwidth)$^{-1}$ is expected with a 100 mA storage-ring current; a beam divergence of less than 20 µrad is also expected. Fig. 1 shows a schematic layout of the beamline. A rotated-inclined double-crystal monochromator (Ishikawa, 1996) equipped with Si(111) crystals is placed 36 m from the source. The energy bandwidth ($\Delta E/E$) is around 2×10^{-4}, which is sufficient for XAFS measurements. A Pt-coated horizontal-beam deflecting mirror is placed 44 m from the source in order to eliminate any residual higher-order undulator radiation. The upstream end of the experimental hutch is 46 m from the source, and the length and height of the hutch are 6.5 and 4 m, respectively. A diamond-crystal phase retarder will be placed at the upstream end of the experimental hutch, which utilizes the phase difference between the in-plane and out-of-plane components of transmitted X-rays around the diffraction condition. Beam attenuation is only caused by absorption through the crystal and further monochromatization or collimation is not necessary. Except for attenuation through the diamond-crystal-monochromated undulator, the beam can be completely used without further monochromatization and collimation. A quarter-wave plate will produce circular polarized X-rays and a half-wave plate will produce vertically polarized X-rays. The orientation of the crystal can be adjusted to maintain a constant phase difference during an energy scan. An X-ray microprobe system is placed on the bench, which can be precisely adjusted to the X-ray beam.

3. X-ray microprobe system for XRF analysis and spectroscopy

Fig. 2 shows a schematic illustration of the XRF microprobe system. The chamber can be evacuated by an oil-free evacuation pump and atmospheric, vacuum and He-filled environments can be selected. A focusing mirror or a glass capillary is used to realize a small-sized X-ray beam on the sample. A spatial resolution of around 5 µm can be realized using a pinhole of 5 µm in diameter attached to the top of a glass capillary, and a spatial

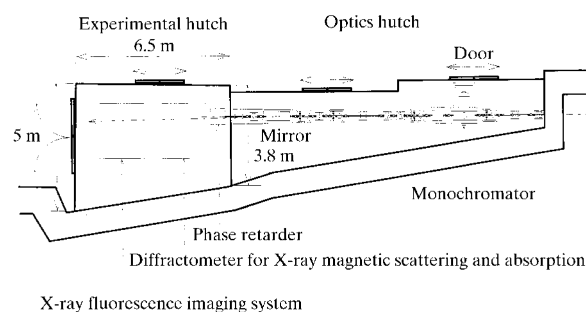

Figure 1
Schematic layout of BL39XU.

© 1998 International Union of Crystallography
Printed in Great Britain – all rights reserved

Table 1
Parameters of the wavelength-dispersive spectrometer.

Bragg angle	21°
Acceptance angle	11.8°
Typical takeoff angle	10°
Typical beam size	5 μm
Spatial resolution of PSPC	200 μm
Sample–detector distance	20 cm
Effective detector area	10 cm (H) × 1 cm (V)

resolution of less than 1 μm is expected with an aspherical focusing mirror. A sample is mounted on the *xyz* and rotational (ψ) stages and the sample can be monitored by an optical microscope and video system. A sample rotational stage will be used to change the takeoff angle of XRF detection. As the practical analysis depth becomes smaller with the smaller takeoff angle geometry the effects of beam divergence on the spatial resolution can be reduced at the expense of signal intensity. Moreover, a smaller takeoff angle geometry defines the analysed volume of the sample as constant during the XAFS measurements and prevents XAFS spectra from spectral distortion (Hayakawa *et al.*, 1991).

To collect XRF signals, both a conventional ED spectrometer using an Si(Li) detector and a wavelength-dispersive (WD) spectrometer with a flat analyser crystal and a position-sensitive proportional counter (PSPC) are attached. These spectrometers can be switched by rotating the sample surface. Although the energy-dispersive spectrometer (EDS) covers a relatively wide X-ray energy range, the upper limit of the counting rate makes it difficult to utilize the flux of the undulator X-rays fully.

3.1. *Wavelength-dispersive XRF spectrometer*

The parameters of the WD spectrometer are shown in Table 1. XRF signals from a sample are dispersed with a flat analyser crystal or a synthetic multilayer, and the dispersed XRF spectrum is detected with a PSPC or an appropriate position-sensitive detector (PSD). By detecting the whole spectrum simultaneously, normalization by the incident beam intensity is not necessary, which is often difficult when the beam is defined by a small pinhole. To cover XRF from 3 to 30 keV, ten analyser crystals can be mounted on a revolver and the spectral region and the resolution can be switched remotely by switching the analyser crystal. The typical energy range detected simultaneously is 6.92 keV (Co $K\alpha$) to 10.53 keV (As $K\alpha$) when using an LiF(200) crystal. The relative energy resolution of the spectrometer ($\Delta E/E$) can be expressed by the following expressions:

$$\Delta E/E = \cot\theta_B \Delta\theta, \tag{1}$$

$$\Delta\theta^2 = \Delta\theta_1^2 + \Delta\theta_2^2 + \omega^2, \tag{2}$$

$$\Delta\theta_1 = d \sin\psi / L, \tag{3}$$

$$\Delta\theta_2 = s/L \tag{4}$$

where θ_B is the Bragg angle, d the beam size on the sample, ψ the takeoff angle (Fig. 2), L the optical path length between the sample and the detector, s the spatial resolution of the PSD and ω the intrinsic width of diffraction; $\Delta\theta_1$ is the angular divergence caused by the finite beam size on the sample and $\Delta\theta_2$ is the angular resolution of the PSD. Fig. 3 shows the energy resolution (ΔE) of this spectrometer as a function of the sample–detector distance for the Cu K–L ($K\alpha$) line with an Si(220) analyser crystal. Since $\Delta\theta$ is mainly determined by $\Delta\theta_2$, the energy resolution can be improved by employing a larger L at the expense of the solid angle of the detector. The present system uses Rigaku delay-line-type vacuum PSPC as a PSD, and its spatial resolution is around 200 μm. Therefore, an energy resolution less than 20 eV is expected at around 8 keV. This energy resolution is sufficient to remove interference of the Ni K–M ($K\beta$) line from the Cu K–L ($K\alpha$) line. To realize higher energy resolution a PSD of better spatial resolution or longer sample–detector distance will be employed.

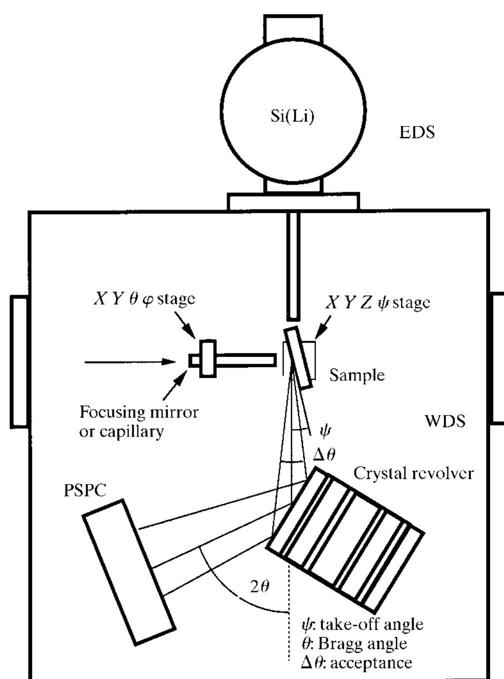

Figure 2
Schematic view of the X-ray microprobe system with wavelength-dispersive and energy-dispersive XRF spectrometers.

4. Research subjects

The following research subjects are being planned to utilize the X-ray microprobe system.

4.1. *Ultra-trace-elemental analysis*

To utilize fully a photon flux of more than 10^{10} photons s^{-1} on samples, a WD spectrometer will be mainly used instead of the ED spectrometer. The advantages of a WD spectrometer are not

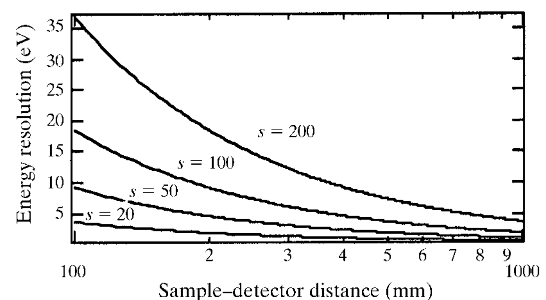

Figure 3
Calculated energy resolution of the wavelength-dispersive spectrometer as a function of the sample–detector distance for the Cu K–L($K\alpha$) line with an Si(220) analyser crystal. The spatial resolution of the detector is represented as s. An intrinsic width of 26.5 μrad, a beam size of 5 μm and a takeoff angle of 10° were used for the calculation.

limited to higher counting rates, but also include a better signal-to-noise ratio. Although the practical solid angle of the WD spectrometer for each XRF line is smaller than that with an Si(Li) detector by a factor of less than 10^{-2}, the minimum detection limit is expected to be less than 100 p.p.b. because of the higher signal-to-noise ratio. The expected detection limit as an absolute amount reaches less than 1 fg or 10^7 atoms for most of the elements covered with this spectrometer.

4.2. *X-ray polarizing microprobe*

The combination of an energy-tunable X-ray microprobe and the phase retarder enables an X-ray polarizing microscope to be made. In the soft X-ray region, circular polarized X-rays are used for magnetic circular X-ray dichroism (MCXD) microscopy and images of magnetic domains have been reported. Considering the relatively large penetration of hard X-rays, MCXD microscopy can be a powerful tool for magnetic materials. Linear polarized X-rays are used to measure the anisotropy of the X-ray absorption spectra and to visualize the domains and structures in polycrystals and aggregated systems.

4.3. *Resonant XRF spectroscopy*

High-resolution measurements of the XRF spectra can provide chemical-state information as peak shifts and as profile changes. Most spectral interpretations depend on the theoretical calculations, and many satellite peaks are attributed to the multiple ionization process by the incident X-rays. By changing the incident X-ray energy around the absorption edge, effects of multiple ionization can be experimentally eliminated. Moreover, many resonant phenomena are expected to be observed. The high-resolution XRF spectrometer also enables selective detection of satellite lines during the XAFS measurements. As reported by Hamalainen *et al.*, (1992) spin-dependent XAFS can be measured by detecting a corresponding satellite line or main line.

We are grateful to Drs Kitamuta and Ishikawa and other SPring-8 staff for providing us with an undulator beamline. We are also grateful for Professors Maruyama and Ito for co-organizing the beamline planning and construction. Many of the beamline components, including the phase retarder, were designed by Drs Suzuki and Kawamura, and all of the spectrochemical analysis group contributed to the design of the system and the planning of the research subjects. This work was partially supported by Grand-in-Aid for Scientific Research No. 08555210 from the Ministry of Education, Science, Sports and Culture of Japan.

References

Hamalainen, K., Kao, C.-C., Hastings, J. B., Siddons, D. P. & Berman, L. E. (1992). *Phys. Rev. B*, **46**, 14274–14277.

Hayakawa, S. & Gohshi, Y. (1996). *Applications of Synchrotron Radiation to Materials Analysis*, edited by H. Saisho & Y. Gohshi, ch. 3. Amsterdam: Elsevier Science.

Hayakawa, S., Gohshi, Y., Iida, A., Aoki, S. & Sato, K. (1991). *Rev. Sci. Instrum.* **62**, 2545–2549.

Hayakawa, S., Iida, A., Aoki, S. & Gohshi, Y. (1989). *Rev. Sci. Instrum.* **60**, 2452–2455.

Hirano, K., Ishikawa, T. & Kikuta, S. (1993). *Nucl. Instrum. Methods*, A**336**, 343–352.

Ishikawa, T. (1996). *SPring-8 Annual Report 1996*, pp. 30–32. SPring-8, Kamigori, Hyogo 678–12, Japan.

Kitamura, H. (1994). *SPring-8 Annual Report 1994*, pp. 47–51. SPring-8, Kamigori, Hyogo 678–12, Japan.

Ohashi, K., Iida, A., Gohshi, Y., Kishimoto, S. & Takahashi, M. (1992). *Adv. X-ray Anal.* **35**, 1027–1033.